11

Optical-Fiber Measurement Systems for Medical Applications

Sergio Silvestri and Emiliano Schena
University Campus Bio-Medico of Rome
Italy

1. Introduction

After telecommunications, also medicine has been revolutionized by optical fibers. They were firstly used, in the early sixties, to visualize internal anatomical sites by illuminating endoscopes. The essential technological solution to obtain good quality images was the introduction of "cladding" during the fifties. The result was the development of minimally invasive tools that have become essential for medical diagnosis and surgery. But optical fibers offer the potential for much more than illumination or imaging tasks. For example, they can also be utilized to sense physiological parameters.

The subject of present chapter is, therefore, a description of the design and measurement principles utilized in fiber optic sensors (FOSs) with a particular reference to biomedical applications.

FOSs development started in the sixties, but the high component costs and the poor interest of the medical community delayed the industrial expansion. The cost reduction of key optical components allowing to realize even disposable or mono-patient FOSs, the increase of components quality, the development of miniaturization, and the availability of plug and play and easy-to-use devices are the main reasons of the growth that is taking place in the use of FOSs.

Moreover, FOSs are characterized by some crucial advantages respect on the conventional transducers that allow to satisfy requirements for use in medical applications: they are robust, may have good accuracy and sensitivity, low zero- and sensitivity-drift, small size and light weight, are intrinsically safer than conventional sensors by not having electrical connection to the patient, large bandwidth, and show immunity from electromagnetic interference. This last feature allows to monitor parameters of physiological interest also during the use of electrical cauterization tools or in magnetic resonance imaging. At present, FOSs are used to measure physical variables (e.g., pressure, force, strain, and fluid flow) and also chemical variables (oxygen concentration in blood, pH, pO_2, and pCO_2).

The simplest FOSs classification is based on the subdivision in intrinsic and extrinsic sensors. In an intrinsic sensor the sensing element is the optical fiber itself, whereas an extrinsic sensor utilizes the optical fiber as a medium for conveying the light, whose physical parameters are, in turn, related to the measurand.

Due to different requirements for miniaturization and safety, in medical applications, these sensors are usually further divided in: invasive sensors, which are inserted into the body,

therefore they must be miniaturized and biocompatible; non-invasive sensors, placed near the body or on the skin surface.
A number of measurement principles can be utilized to realize transducers based on the variation of fiber optic properties with physical or chemical variables, or based on variation of light parameters in the fiber. As the wide variety of techniques developed to design FOS for medical applications, just some of them are here described in detail.
This chapter is divided into subsections where a concise description of the measurement principle of FOSs is presented along with the main medical applications. Particular emphasis is placed on the metrological characteristics of the described FOSs and on the comparison with conventional sensors. Measurement principles include interferometry-based, intensity-based, fiber Bragg grating and laser Doppler velocimetry sensors.
In the following sections, the four abovementioned working principles and their use in specific medical applications to sense variables of physiological interest are investigated. The performances of the sensing methods are also presented with particular reference to the description of commercially available sensors.

2. Interferometry-based and intensity-modulated fiber optic sensors

FOSs can be realized with a working principle based on a large number of interferometric configurations, e.g., Sagnac interferometer, Michelson interferometer, Mach-Zehnder interferometer, and Fabry-Perot interferometer (Yoshino et al., 1982a) (Davis et al., 1982). Typically, these approaches show an extremely high sensitivity although cross-sensitivity represents a significant drawback: first of all the influence of temperature may introduce quite high measurement uncertainties (Grattan & Sun, 2000).
These FOSs can be designed as intrinsic sensors, where the sensing element is the fiber itself, or as extrinsic sensors, where a small size sensing element is attached at the tip of an optical fiber. The most common configuration is the second, where the sensing element, placed at the tip of the optical fiber, causes changes of light parameters in a well-known relation with the measurand. In this case, the optical fiber is employed to transmit the radiation emitted by a light source (e.g., laser or diode) and to transport the radiation, modulated by the measurand, from the sensing element to a photodetector (e.g., an optical spectrum analyzer). Thanks to this solution, the sensor can be used also for invasive measurements, as the largest part of the measurement system (light source and photodetector) can be placed far from the miniaturized sensing element, due to the very limited energy losses of light in the fiber.

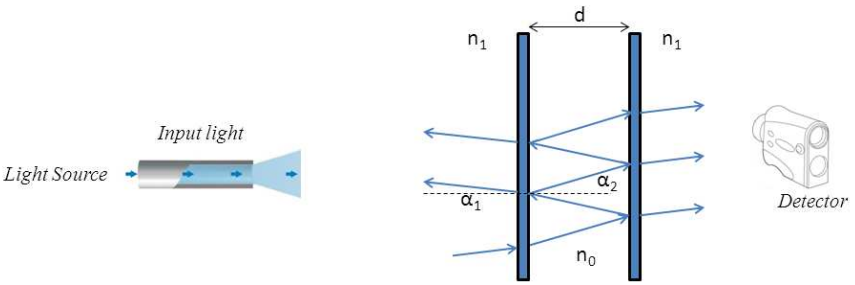

Fig. 1. Schematic representation of a Fabry-Perot interferometer.

In medical applications, mainly dedicated to force and pressure monitoring (Rolfe et al., 2007), the most common design is based on the interferometer configuration proposed by Fabry and Perot (Fabry & Perot, 1898), also known as multi-beam interferometer because many beams interfere in one resonator. A typical realization is composed of two parallel high reflecting mirrors placed at distance *d* (Figure 1). If *d* is variable, the instrument is called a Fabry-Perot interferometer. If *d* is fixed, whereas the incident light angle varies, the instrument is called a Fabry-Perot etalon. The Fabry-Perot interferometer allows to distinguish very close radiation wavelengths.

The Fabry-Perot cavity is usually utilized as secondary element of the sensor. Its output is an electromagnetic radiation with a wavelength that is function of *d*. In order to have high performances a measurement system based on Fabry-Perot interferometer needs a photodetector discriminating radiations with very close wavelengths. The working principle can be described as follows. When a light beam, emitted by a light source (e.g., a laser), enters between the two mirrors, a multiple reflections phenomenon takes place. The electromagnetic waves in the cavity can interact constructively or destructively, depending on if they are in phase or out of phase respectively. The condition of constructive interference, corresponding to a peak of transmitted light intensity, happens if the difference of optical path length between the interacting beams is an integer multiple of the light wavelength. The phase difference between interacting beams, and therefore the intensity of transmitted light, depends on the distance *d* between the mirrors. Considering for simplicity the same value for the refractive index upward the first surface and downward the second mirror (n_1), the intensity of transmitted light can be expressed as follows (Peatross & Ware, 2008):

$$I = I_0 \cdot \frac{(1-R)^2}{(1-R)^2 + 4 \cdot R \cdot \sin^2\left(\delta/2\right)} = I_0 \cdot \frac{1}{1 + F \cdot \sin^2\left(\delta/2\right)} \tag{1}$$

Where I_0 is the intensity of the incoming wave, F is the cavity's coefficient of *finesse* that can be expressed by the following equation:

$$F = \frac{4 \cdot R}{(1-R)^2} \tag{2}$$

R is the reflectance of both mirrors, and δ, the phase difference between each succeeding reflection, is a function of the radiation wavelength (λ), the distance between the two mirrors (*d*), and the angle between the radiation direction and the normal to the mirror surface (α_1):

$$\delta = \frac{4 \cdot \pi \cdot d \cdot n_1}{\lambda} \cdot \cos\alpha_1 \tag{3}$$

In order to increase the sensitivity of the Fabry-Perot interferometer, it is desirable that the intensity (I) varies strongly with δ. Equation 1 shows that sensitivity of I with δ increases when F is increased. Therefore, the sensitivity of the device increases when F, and consequently R, is increased, as shown by equation 2. For the above mentioned reasons, important parameters of a Fabry-Perot interferometer are: the difference between two succeeding transmission peaks (free spectral range) and the value of R. In fact, the difference between the maximal and the minimal peaks of the transmitted radiation increases with R,

moreover, the trend of I as a function of *d* becomes sharper when R increases: this makes easier the determination of *d* variations. A mirror with a very high reflectance (R) is usually obtained by coating the internal surface of the two mirrors.

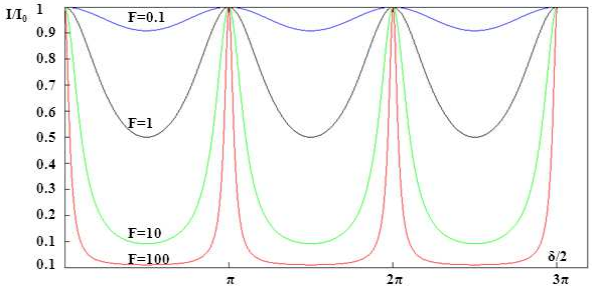

Fig. 2. Ratio between the intensities of transmitted and incident radiation as a function of δ/2 for different values of cavity's finesse coefficient.

Figure 2 shows the ratio between the intensity of transmitted and incident light as a function of δ/2, considering a normal incident radiation ($\cos\alpha_1 \approx 1$), for the following F values: F=0.1 (R≈2.4 %), F=1 (R≈17 %), F=10 (R≈54 %), F=100 (R≈82 %).

Thanks to the use of an optical fiber coupled to a Fabry-Perot cavity, the measurement system can be miniaturized, with the light source and the photodetector separated from the sensing element (the cavity). Moreover, the small size of the sensing element, along with the flexibility of the fiber optic with small outer diameter, allows to directly insert the sensing element into the body for use in clinical applications where an invasive measurement is required. Some sensors, showing the above described working principle, designed for medical applications are reported in Section 2.1.

The intensity-modulated FOSs are characterized by a working principle based on the intensity variation of the reflected light into the fiber related to a displacement induced by the measurand on a secondary element. A basic configuration shows one or more optical fibers with the extremity placed at a known distance from a movable mirror having high reflectance. The radiation, emitted by a source and conveyed into the fiber, is reflected by the mirror: the distance (*d*) between the fiber tip and the mirror is related to the measurand magnitude. The intensity of the back-reflected light coupled to the fiber is a fraction of the incident light intensity and depends on the distance between the fiber and the reflecting surface, or on a deformation of the surface: an increase of the distance causes a decrease of the back-reflected intensity as shown in figures 3a, 3b, and 3c. This principle, when applied to a secondary transducer, allows to measure several physical variables: temperature, pressure, force, fluid velocity and volumetric flow rate.

More complex configurations have been realized with solutions improving sensor performances (Puangmali et al., 2010).

Other methods applied to the design of intensity-modulated FOSs are based on the light coupling of two fibers (Lee, 2003). In this configuration, schematically reported in figure 4, the radiation emitted by a light source is conveyed within a fiber optic, whose distal extremity is placed in front of another fiber. The intensity of the light transmitted into the second fiber, and measured by a photodetector placed at its distal tip, is related to the distance (*d*) between the two fiber tips: the transmitted intensity decreases when *d* increases,

as shown in figures 4a, 4b, and 4c. The measurand can be a displacement or a physical variable causing the displacement, such as force, pressure or temperature.

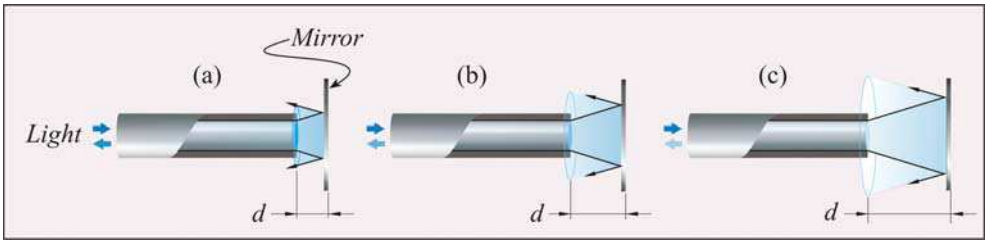

Fig. 3. Schematic representation of common intensity-modulated FOSs realized with a fiber and a reflecting surface. The intensity of the reflected radiation coupled to the fiber at different distances d between the fiber and the mirror (a, b, and c).

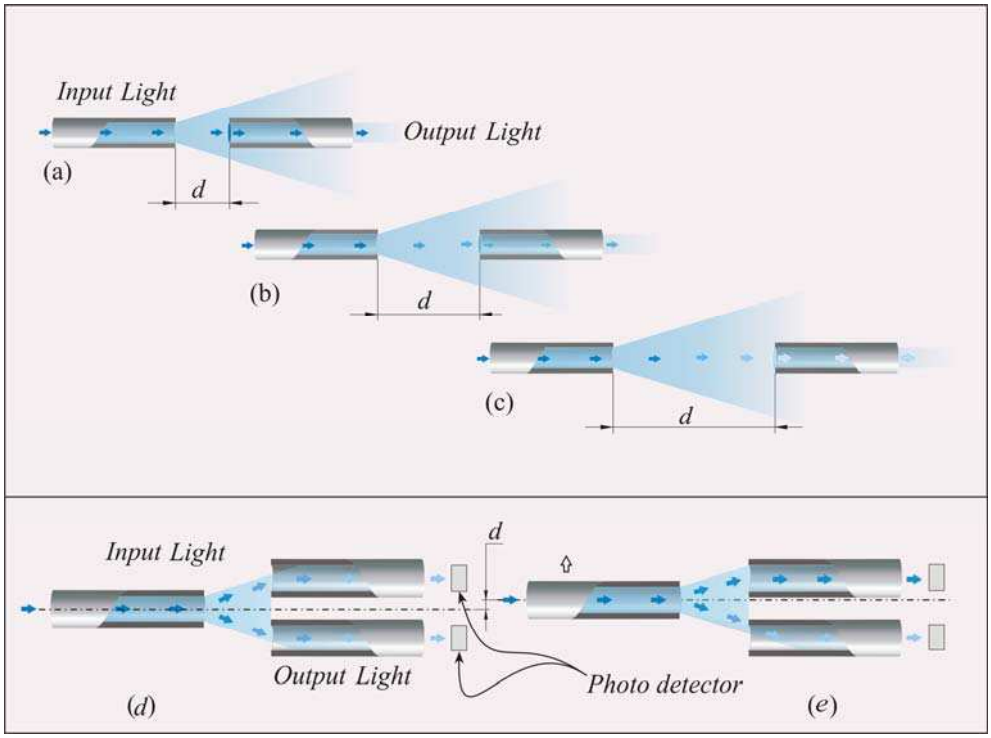

Fig. 4. Schematic representation of intensity-modulated FOSs realized with two fibers or more. The intensity of the coupled radiation of the two fibers is function of their distance *d*: if *d* increases the intensity of collected light decreases (a, b, and c). Sensors' performances can be improved using differential configuration (d, and e).

The above described configuration can be improved using three or more fibers in differential configuration for the compensation of changes in the light source intensity or losses in the fiber, as shown in figure 4d and 4e.
An interesting example of sensor designed with this working principle is a flow-meter based on the vortex shedding phenomenon: the light intensity transmitted between the fibers is modulated by the periodical mechanical motion caused by vortex shedding. The light intensity is converted by a photodiode in an electric signal related to the flow rate. This sensor can be used to perform measurements of fluid flow rate also at high temperature (350 °C) (Wroblewski & Skuratovsky, 1985).
A further design to realize intrinsic intensity-modulated FOSs is based on microbending. The bending of an optical fiber, in fact, causes an attenuation of the light intensity conveyed. As it is well known, the ever-present radiation loss into the cladding region causes an attenuation when the light passes through a fiber. The intensity loss into the cladding region can be increased if the fiber is bent (figure 5). Also this working principle allows to sense pressure, force, fluid velocity and volumetric flow rate.

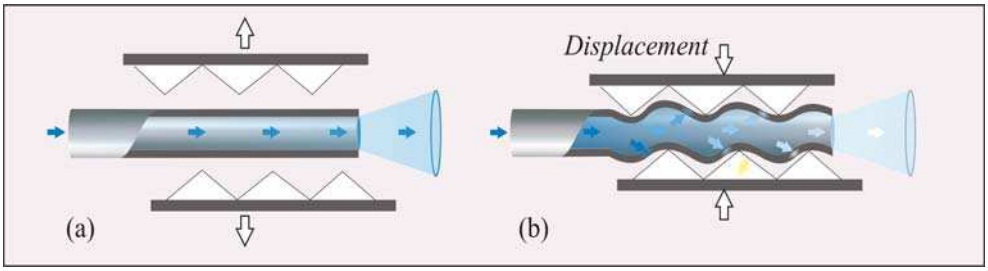

Fig. 5. a and b: principle of work of FOS based on microbending that transduces a displacement causing the bending into an intensity attenuation.

Generally speaking, intensity-modulated FOSs are characterized by the main advantage of requiring a modest amount of electronic interfaces (Udd, 2006).

2.1 Interferometry-based and intensity-modulated fiber optic sensors: medical

Intracranial pressure (ICP) is the cerebrospinal fluid pressure inside the skull. Being the skull a rigid case, any volumetric increase of its content may raise the ICP. The ICP monitoring is probably the most important application of FOSs in the medical field at the moment. During the sixties there was a significant propulsion in the development of pressure FOSs for measurement of intravascular blood pressure (Lekholm & Lindstrom, 1969) and in the early seventies some patents were issued describing FOSs to measure the ICP.
The ICP value is principally due to two main components: cerebrospinal fluid (CSF) volume, that is responsible for ICP baseline and can cause, in pathological conditions, an increase of this parameter; vasogenic components causing small fluctuations of cerebral blood volume, that can increase the ICP value in conditions of hypercapnea or increase of cerebral metabolism. Mass lesions (tumors, pus or hematoma), vascular engorgement (e.g., in case of traumatic brain injury), cerebral oedema or hydrocephalus may also increase the ICP value.
Its monitoring is, therefore, essential in patients with traumatic brain injury, tumors or pus, where the ICP increase is a common cause of ischemia, intracranial hemorrhages or brain

herniation. Since the ICP value varies continuously, an uninterrupted record of the ICP should be obtained in order to avoid the loss of diagnostic data.
Normal ICP values depend on age, position and clinical conditions. In supine position it ranges from 7 mmHg to 15 mmHg for adults and from 3 mmHg to 7 mmHg for children; an ICP exceeding 20 mmHg needs therapeutic treatment (Smith, 2008).
Although some attempts have been performed to introduce non-invasive or minimally-invasive methods, e.g., the estimation of ICP by the measurement of tympanic membrane displacement (Shimbles et al., 2005) or by ultrasound-based techniques (Yoshino et al., 1982b), the ICP monitoring usually requires invasive transducers. Transducers can be placed in parenchymal, ventricular, epidural, subdural, or subarachnoid locations, although measurements obtained from the last three sites appear less accurate (Bratton et al., 2007). Also, lumbar puncture can be utilized to estimate the ICP, but this indirect measurement not always correlates with the ICP value. In the clinical practice, the monitoring is performed in several ways: 1) through a catheter placed in ventricular, epidural or subarachnoid spaces and connected to an external strain gauge; 2) through a micro strain gauge typically placed in ventricular or parenchymal catheters; 3) through FOSs guided inside the ventricles, brain parenchyma, subdural or subarachnoid spaces.
The standard proposed by the Association for the Advancement of Medical Instrumentation (AAMI) provides the performances that a device intended for ICP measurement should assure. The device should have a pressure range between 0 mmHg and 100 mmHg, an accuracy better than ±2 mmHg in the range from 0 mmHg to 20 mmHg, and lower than 10 % of the measured value in the range from 20 mmHg to 100 mmHg (Bratton et al., 2007).
Commercially available FOSs, intended to monitor ICP value, are based on two working principles. The former was introduced by T. E. Hansen, who described an interesting micro-tip FOS for medical applications (Hansen, 1983). Successively, A. Lekholm and L. Lindstrom realized a FOS with the same measurement principle for intravascular use (Lekholm & Lindstrom, 1969) and A. Wald dedicated it to monitor the ICP (Wald et al., 1977). The working principle is based on the presence of two groups of fiber bundles connected to a LED and to a photodetector respectively. At the common end of the bundle is placed a thin metal membrane reflecting the light. In this way, the light emitted by LED is conveyed to the fibers connected to the photodetector, as schematically reported in figure 6.

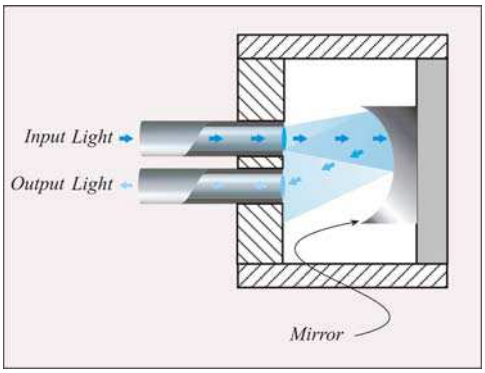

Fig. 6. Schematic representation of the sensing element of the FOS made by Camino Laboratories: the output light variation is related to the pressure that causes a mirror displacement.

The coupling and, therefore, the photodetector signal, depends on the membrane deflection caused by an external pressure. These FOSs have small size, e.g., an outer diameter of 1.5 mm or 0.85 mm for the unshielded case, and a frequency response flat from 0 Hz up to 15 kHz. On the other hand, they show zero drift if a temperature step from 20 °C to 37 °C is applied, recovering the baseline after about 40 s.

The second FOS design is based on Fabry-Perot interferometry (Fabry & Perot, 1898). These sensors were introduced in the late seventies (Mitchell, 1989). The sensing element shows two parallel optical reflecting surfaces, as schematically reported in figure 1, and one of them is a pressure sensitive diaphragm. A variation of the external pressure causes a deflection of the diaphragm, reducing the optical cavity depth. The optical cavity is, therefore, with variable dimension allowing light intensity curve having multiple *maxima* and *minima* that depend on cavity depth.

At present, some fiber optic devices based on micro-optical mechanical systems (MOMS) to monitor the ICP are commercially available.

FISO Technologies, Inc. has developed some pressure FOSs for medical applications constituted by a Fabry-Perot cavity whose optical length changes with the physical parameters to be measured. The FOP-MIV pressure sensor is a miniaturized Fabry-Perot cavity constituted by a micromachined silicon diaphragm membrane, acting as pressure sensing element (Chavko et al., 2007). When pressure increases, the thin membrane is deflected and the Fabry-Perot cavity depth is reduced, in this way the small cavity depth variations are related to pressure variations. Vacuum inside the cavity prevents changes of internal pressure caused by gas thermal expansion that would, otherwise, distort the pressure measurement.A high vacuum is maintained inside the cavity therefore, the FOP-MIV measures absolute pressure. Being one of the smallest pressure sensors commercially available, FOP-MIV is well designed for many medical applications where size is an important issue (Hamel & Pinet, 2006). The optical nature of the FOP-MIV, makes the sensor immune to electromagnetic field or radiofrequency interferences regularly encountered in operating rooms or MRI environment. FOP-MIV is characterized by a measurement range up to 300 mmHg, an accuracy equal to 1.5 % of full scale output (or ±1 mmHg), a resolution better than 0.3 mmHg, a thermal effect sensitivity of 0.1 %/°C; a zero drift thermal effect of 0.4 mmHg/°C.

Innerspace, Inc. produces a device to monitor ICP also based on the Fabry-Perot cavity: the pressure, deflecting the diaphragm, alters the cavity depth and thus the optical cavity reflectance at a given wavelength. If a LED source is used, the spectrally modulated reflected light can be split into two wavebands by a dichroic mirror. The ratio of the two signals provides a pressure estimation immune to the typical light level changes occurring in FOS systems. The measurement range is from -10 mmHg up to +100 mmHg, the linearity and hysteresis is ±2 mmHg from 0 mmHg to 10 mmHg and 10% of reading from -10 mmHg to 125 mmHg (Mignani & Baldini, 1995).

Camino Laboratories realized the ICP monitoring through an intensity-modulated based FOS. A dual-beam reference, using a secondary fiber optic path, is joined to the pressure measuring fiber link, but unaffected by pressure variations. The sensor is based on the intensity modulation technique with dual-beam referencing. The radiation conveyed within a fiber optic is coupled to a fiber by a bellow with a reflecting surface. The intensity of the coupled radiation depends on the position of the bellow's tip, which is function of the pressure, as shown in figure 6. The measurement range is from 0 mmHg up to 100 mmHg, linearity and hysteresis is ±2 mmHg from -10 mmHg to +50 mmHg and 6% of read value

from +50 mmHg to +125 mmHg, the frequency response shows an attenuation of -3dB from 33 Hz to 123 Hz, a zero drift <2 mmHg (first 24 hours) and less than 1 mmHg/day (first 5 days).

At present, the "gold standard" technique for ICP monitoring is considered a catheter inserted into the lateral ventricle and connected to an external strain gauge (Smith, 2008). The main advantages include the chance to perform a periodic external calibration and a slightly lower cost than microstrain gauge and fiber optic devices (Bratton et al., 2007). However, also these sensors have their own set of potential complications, including obstruction or disconnecting of the tubing, occasional difficulties to place in the presence of brain swelling and shift (Ostrup et al, 1987), migration of the catheter out of the ventricle (Al-Tamimi et al., 2009), and infections occur in up to 11% of cases (Steiner & Andrews, 2006). Microstrain gauge and FOS show similar metrological characteristics but with a higher cost. The additional advantages of FOS devices are: the immunity to the electromagnetic interferences that allows to monitor the ICP during magnetic resonance or during the use of electrical cauterization tools, no obstruction and electrical hazard, and a quite low zero-drift (Crutchfield et al., 1990).

Arterial pressure invasive measurements can also be performed through FOSs. The most widely used configuration is Fabry-Perot interferometry. Many studies describe miniaturized pressure sensors (Ceyssens et al., 2008; Totsu et al., 2005). FOS allows to obtain a large bandwidth (some kHz), an accuracy better than 4 % of the read value, and a measurement range that covers the physiological pressure values (less than 300 mmHg).

Wolthuis *et al.* developed a Fabry-Perot FOS able to perform a concurrent measurement of pressure (with resolution of 1 mmHg, measurement range from 1 mmHg to 1000 mmHg and flat frequency response up to 1000 Hz) and temperature (with resolution of 0.2 °C, rise time of 20 ms, and measurement range from 10 °C to 60 °C) (Wolthuis et al., 1993). RJC Enterprises, LLC realized further developments of the sensor using the same principle of measurement. For temperature measurement, the outer surface of a thin silicon layer defines the optical reflecting cavity; the refractive index of silicon changes with temperature altering the optical cavity reflectance spectra The transducer (for pressure and temperature) contains a 850 nm LED whose emission reaches the sensor via an optical fiber. In the sensor's optical reflecting cavity, the spectral distribution of the LED light is modified as a function of cavity depth, and this spectrally altered light is reflected back down the fiber to the instrument. Light returning to the instrument is optically split into two spectral components; the photocurrents from these two components form a ratiometric signal which in turn correlates with changes in the measured parameter (Wolthuis et al., 1993). The sensor shows some advantages: small size (the maximum dimension is 300 μm), resolution of 0.02 °C and 0.1 mmHg, accuracy of 0.1 °C and ±1 mmHg (or 2 % of read value), bandwidth up to 500 Hz limited only by supporting instrumentation, measurement range from 15 °C to 55 °C and from 500 mmHg to 1100 mmHg (absolute pressure).

An interesting application of these sensors is related to the intra-aortic balloon pumping (IABP) therapy, which is a therapy of circulatory support often used to help patients recovery from critical heart diseases, cardiac surgery or to wait until a transplant is performed. A catheter, terminated by an inflatable balloon, is introduced through the femoral artery and is positioned into the descending aorta just below the subclavian artery. The inner lumen of the catheter can be used to monitor systemic arterial pressure and the outer lumen is used for the delivery of gas to the balloon. The balloon must be rapidly inflated with the onset of the diastole and deflated when the systole happens. The

synchronization between the balloon pumping and the heartbeat can be done either by using electrocardiogram (ECG) signals or aortic-pressure waveform (Trost & Hillis, 2006). The second approach is required when ECG signals are distorted or unavailable (Dehdia et al., 2008). FOSs are used to measure blood pressure, so that to give a trigger to the balloon. The traditional technique to monitor the aortic pressure is performed by an external electrical sensor, which measures pressure applied through a fluid-filled catheter. Many drawbacks are associated with this method such as, among others, the damping effects due to catheter elasticity or the presence of air micro-bubbles and the presence of catheter vibrations. These drawbacks are eliminated by the use of a FOS mounted at the tip of the catheter. It also shows a good accuracy and resolution, and a large bandwidth. Moreover, it is miniaturized (MOMS) decreasing the risk of ischemia, that is the main risk associated with IABP therapy (Pinet, 2008).
FISO Technologies, Inc has developed a pressure FOS for this application constituted by a Fabry-Perot cavity. The working principle has been presented in the previous section. Thanks to the small size (diameter of 550 μm) the sensor shows a large bandwidth limited by the signal conditioner at 250 Hz, the resolution is 0.5 mmHg (Pinet et al., 2005). Coupling this sensor with a faster signal conditioner could result in a better dynamic response of traditional catheter tip pressure sensor and can be used in presence of strong EM fields (e.g., during magnetic resonance investigation).
FOS is also used in IABP therapy by Arrow International, Inc. and by Maquet Getinge Group. It shows an accuracy of 4 mmHg or 4 % of read values whichever is greater, and a pressure range from 0 mmHg to 300 mmHg.
Opsens produces a FOS with the same working principle to monitor blood pressure. Small size (catheter diameter equal to about 250 μm), pressure range from -50 mmHg to +300 mmHg, and good resolution (0.5 mmHg) and accuracy (0.5 mmHg or 1 % of full scale) are the main advantages. It can also be used to monitor ICP and urodynamic pressure.
FOSs based on Fabry-Perot interferometry are also used to perform direct measurements of intra-tracheal pressure. Direct intra-tracheal pressure measurements show some advantages to monitor respiratory mechanics. This measurement is usually performed by introducing a catheter into the endotracheal tube (ETT) and connecting it to a conventional pressure transducer. In pediatric respiratory monitoring this approach is usually not performed because it implies an excessive occlusion of the narrow pediatric tubes (Guttmann et al., 2000). Samba Sensors designs a FOS for intra-tracheal pressure monitoring. It consists of a membrane that changes the depth of a microcavity with pressure (Fabry-Perot interferometry). It shows some advantages such as: small size (the silicon sensor chip diameter is equal to 420 μm, the fiber optic diameter is 250 μm or 400 μm), measurement range between -50 cmH_2O and +350 cmH_2O, low temperature drift (< 0.2 cmH_2O/°C), accuracy of 0.5 cmH_2O or 2.5 % of reading between -50 cmH_2O to +250 cmH_2O and 4 % of reading between +250 cmH_2O to +350 cmH_2O, short response time (1.3 ms), moreover the introduction of the sensor into the ETT does not significantly increase the fluid-dynamic resistance, therefore the pressure drop across the ETT (Sondergaard et al., 2002). This company produces another FOS, with similar metrological characteristics of the above described sensor, used in urology to monitor bladder pressure and the pressure in the lower urinary tract, especially important in paraplegic patients for the high risk of urinary tract infections.
An interesting application of intensity-based FOSs was presented by Babchenko *et al*. They performed the measurement of the respiratory chest circumference changes (RCCC) through

a bending-based FOS composed of a bent optic fiber connected to the chest so that its curvature radius changes during respiration due to RCCC. The light intensity transmitted through the fiber depends on the bent, so that provides an indirect measurement of the RCCC (Babchenko et al., 1999).

3. Fiber Bragg grating sensors

About thirty years have passed since the introduction of fiber Bragg grating (FBG) sensors, when Hill *et al*. discovered the phenomenon of photosensitivity (Hill et al., 1978). They discovered that an optical fiber with a germanium-doped core can show a light-induced permanent change in the core's refractive index thanks to an electromagnetic wave with high intensity and a particular wavelength. An optical fiber core characterized by periodic refractive index changes constitutes a FBG. Only eleven years later, a milestone study describing a FBG-based sensor was published (Meltz et al., 1989). The development of such sensors was mainly delayed due to the high cost and the realization difficulties, that only during the nineties showed a considerable reduction. Nowadays, there are two main techniques to realize fiber grating: interferometric and phase mask method. These techniques allow for the manufacturing of some different types of grating classified as: FBG; long-period fiber grating; chirped fiber grating; tilted fiber grating; and sampled fiber grating (Lee, 2003). The gratings are called fiber Bragg gratings (FBGs) if the grating spatial period has the order of magnitude of hundreds of nanometers, or long period gratings (LPGs) if the spatial period has the order of magnitude of hundreds of micrometers.

FBG sensors are characterized by a working principle based on the coupling of the forward propagating core mode to the backward propagating core mode. When light propagates through a fiber with a Bragg grating, a phenomenon of radiation reflection happens only for a narrow range of wavelengths, other wavelengths are transmitted. The wavelength placed in the middle of the reflected range is called Bragg wavelength λ_B, and can be expressed by the following equation:

$$\lambda_B = 2 \cdot n_{eff} \cdot \Lambda \tag{4}$$

where Λ is the spatial period of the grating, and n_{eff} is the effective refractive index of the fiber core.

The working principle, commonly used in FBG sensors, is based on λ_B shift due to a variation of the spatial period of the grating, or on λ_B shift due to a refractive index variation of the core, as shown in equation 4. The former is the technique typically implemented to perform strain measurement; the second is mainly used to monitor changes of temperature, as a consequence of the temperature influence on n_{eff}. As the measurand directly modulates the signal into the fiber, FBGs are examples of fiber optic intrinsic sensors.

Figure 7 shows the λ_B shift from λ_{B1} to λ_{B2} caused by a strain.

Therefore, the relative variation of the Bragg wavelength can be expressed as a function of the fractional changes of the spatial period and of the effective refractive index:

$$\frac{\Delta\lambda_B}{\lambda_B} = \frac{\Delta\Lambda}{\Lambda} + \frac{\Delta n_{eff}}{n_{eff}} \tag{5}$$

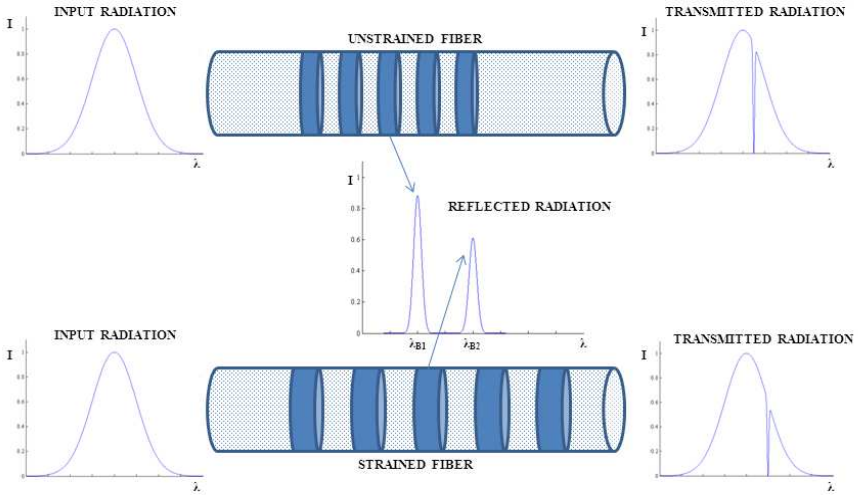

Fig. 7. Shift of Bragg wavelength due to fiber optic strain.

The relative λ_B change can be also expressed showing its dependence on the fiber strain, ε, and on the temperature variation, ΔT:

$$\frac{\Delta\lambda_B}{\lambda_B} = P_e \cdot \varepsilon + \left[P_e\left(\alpha_s - \alpha_f\right) + \varsigma \right] \cdot \Delta T \tag{6}$$

where P_e is the strain-optic coefficient, α_s and α_f are the thermal expansion coefficients of the fiber bonding material and of the fiber respectively, and ς is the thermo-optic coefficient (You & Yin, 2002). In the environmental temperature range, for a silica fiber, the thermal effect is dominated by the effect of temperature changes on n_{eff} (dn_{eff}/dT) that is one order of magnitude greater than the effect of thermal expansion. In fact, about 95% of the wavelength shift is caused by the effect of temperature changes on n_{eff}.
FBG response (shift of λ_B) for strain input and temperature changes depends on λ_B and FBG types (Shu et al., 2002). Typical strain sensitivities are: 0.64 pm/με at λ_B near to 830 nm; 1 pm/με at λ_B near to 1300 nm; 1.2 pm/με at λ_B near to 1550 nm. Typical temperature sensitivities are: 6.8 pm/°C at λ_B near to 830 nm; 10 pm/°C at λ_B near to 1300 nm; 13 pm/°C at λ_B near to 1550 nm (Rao, 1998).
Although the effect of one of the two components on λ_B shift is predominant, both components can be separated through the implementation of specific configurations, e.g., a reference FBG added to the main sensor (Xu et al., 1994), in order to attenuate the influence of the undesired effect and to improve the repeatability of the measurement system.
As these sensors can detect physical variables such as strain, temperature, force, pressure, vibrations, they have been widely utilized for clinical applications in some medical fields, described in detail in the following section.

3.1 Fiber Bragg grating sensors: medical applications

Although this technology is characterized by a high potential for the monitoring of diagnostic variables thanks to the immunity of electromagnetic field, the non-toxicity, the possibility of realizing miniaturized sensors, the biocompatibility, and it has been

introduced in researches for medical application for more than 20 years, it is not yet widely used in clinical practice (Mishra et al., 2011).
In the late nineties Rao *et al.* described a FBG-based system for medical applications (Rao et al., 1998). In particular, they developed two temperature sensors: the former was used for cardiac monitoring estimating the stroke volume with thermodilution technique, the second one was realized for *in vivo* blood temperature monitoring. In both cardiac output and blood temperature monitoring the use of FBG-based sensors allows to substitute traditional sensing elements that are electrically active or powered, therefore poorly appropriate where high electro-magnetic fields are present or in some other medical applications. These sensors were also used to monitor heart muscle activity: the sound generated by the heartbeats causes vibrations of a membrane. The stretches and contractions of the FBGs, mounted on the membrane, can perform vibrations measurement (Gurkan et al., 2005).
FBG was also used for other interesting medical applications. One of them is related to the invasive ablation treatment of Atrial Fibrillation (AF). AF is a cardiac arrhythmia that typically causes poor heart blood pumping. There are two treatments for AF: pharmaceutical drugs and electrical defibrillation (cardioversion), and invasive ablation surgery. Surgical ablation is performed by, among many methods, radiofrequency (RF) waves conveyed in an invasive probe. Some studies show that lesion size, caused by RF ablation, is related to electrode-tissue contact force (Haines, 1991). The strong influence of contact force on the amount of the ablated tissue shows the importance of its monitoring. A FBG-based sensor has been developed to perform a real time monitoring of the contact force (Yokoyama et al., 2008). The sensor (TactiCath, Endosense SA), incorporated in the ablation catheter, is composed of three optical fibers to monitor the deformation of the catheter tip. Three FBGs, mounted on the deformable body, allow to relate the body deformation with the applied force representing the above mentioned contact force between the ablation catheter and the tissue. An infrared laser radiation (wavelength ranging from 1520 nm to 1570 nm) conveyed in three fibers is partially reflected at a particular wavelength (λ_B) related to the body deformation, so that to the contact force. This system allows to measure contact force along three different directions (parallel, perpendicular, and at 45° with the tissue) at frequency of 10 Hz, the discrimination threshold is better than 10^{-3} kgf ($9.8 \cdot 10^{-3}$ N), a further advantage is the small size (catheter tip diameter equal to 3.5 mm).
FBG-based force transducers could play an important role in minimally invasive surgery (e.g., laparoscopic surgery widely used in appendectomy, stomach surgery, surgery of the colon and of the rectum) or in minimally invasive robotic surgery (e.g., Da Vinci), to provide a feedback of the forces applied to the tissue during the surgery. The force monitoring allows to minimize the tissue damage (Song et al., 2009). Microsurgery is characterized by a wide number of applications for FBG-based sensors. Sun *et al.* realized a FBG-based sensor to monitor force between tool and tissue during retinal microsurgery (Iordachita et al., 2009). In this application, the force monitoring can help the surgeon, since the intensity of interaction forces is usually lower than human perception. The sensor is characterized by: good resolution (0.25 mN) that allows to monitor very low forces, and a temperature compensation through the use of a further reference FBG that improves the sensor repeatability.
During alternative surgical technique for tumors removal, as laser-induced thermotherapy (LITT), FBG sensors could result useful. LITT destroys the neoplastic tissues inducing hyperthermia through laser light delivered through optical fiber probe placed in correspondence of the tumor. During the LITT treatment, the monitoring of tissue temperature could avoid inefficacy in the treatment caused by excessive temperature values

of the tissue, that can cause the damage of the healthy tissue close to the neoplastic one, or to low temperature values that can cause an incomplete ablation of the neoplastic tissue. FBG sensor with spatial resolution of 0.25 mm has been designed to monitor the tissue temperature during LITT (Li et al., 2009) and to use its value to control the temperature in the boundary region at 35 °C to improve the safety of the LITT treatment (Ding et al., 2010), *in vivo* measurements during this procedure are also performed (Webb et al., 2000).

4. Fiber optic sensors for laser Doppler velocimetry

Generally speaking, the design of these sensors is based on the "Doppler shift" described by Christian Doppler in 1842 in an article entitled "On the colored light of double stars and some other heavenly bodies". If an electromagnetic or acoustic wave is reflected back by a moving object, it undergoes the Doppler shift phenomenon, i.e., the frequency of the reflected wave is different from the frequency of the incident one. This frequency difference is related to the speed of the moving object and can be expressed by the following relation (Beckwith et al., 1995):

$$\Delta f = \left(\frac{2V}{\lambda}\right) \cdot \cos\beta \cdot \sin\left(\frac{\alpha}{2}\right) \tag{7}$$

being V the moving object speed, λ the wavelength of the incident wave, α the angle between the axis of the incoming wave and the observer, and β the angle between the moving object velocity direction and the bisector of the angle between the axis of the incoming wave and the segment connecting the object and the observer, as shown in figure 8.
If the object moves within a fluid flow, its velocity can be approximately equal to the average velocity of the fluid flow, therefore the frequency shift measurement becomes an indirect measurement of the flow rate.

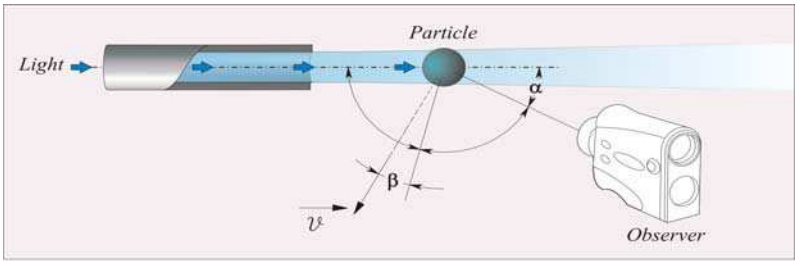

Fig. 8. By illuminating a moving particle with the light transported through a fiber, a frequency variation of the light reaching the observer is obtained.

The performances of these sensors have been improved through the dual-beam approach, a schematic representation is depicted in figure 9.
The radiation is split into two beams, through a beam splitter, successively crossed into an intersection region through a mirror. This region defines a sampling volume, placed into the fluid flow, where the particle velocity is measured. In the intersection region, an interference pattern, characterized by alternating interference fringes, is produced. When a particle passes through the fringes, it causes periodic variations of the intensity of the scattered light.

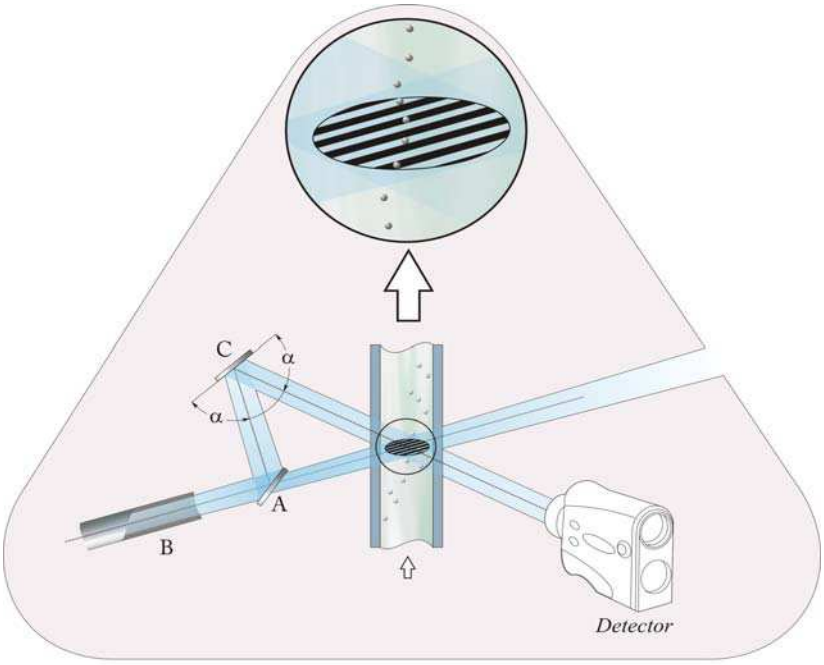

Fig. 9. Schematic representation of the working principle of FOS based on laser Doppler differential approach and its components: the beam splitter (A), the fiber optic (B), the mirror (C).

The light intensity time plot, monitored by a photodetector, reports these periodic variations and allows to estimate the flow rate.
The particle speed (V) is related to the frequency fluctuations (fr) of the scattered intensity and to the distance between two contiguous fringes (γ) as follows:

$$V = \gamma \cdot f_r = \frac{\lambda}{2 \cdot \sin\left(\frac{\theta}{2}\right)} \cdot f_r \tag{8}$$

where θ is the angle between the two beams.
The use of fiber optics to transmit the incident and the reflected light enhances the chances to perform both invasive and non-contact measurements allowing for monitoring very low flow rates, such as blood flow in capillaries: the use of light waves instead of sound waves allows to estimate the speed of red blood cells when they moves into the capillaries. A detailed description of the medical applications is reported in the following section.

4.1 Laser Doppler velocimetry: medical applications

Laser Doppler velocimetry (LDV) sensors in medical arena are used to perform measurements of blood flow rate in some tissues, i.e., perfusion. As the perfusion is a primary parameter in the local transport of oxygen, nutrients, heat, *et cetera* its monitoring is useful in several diagnoses. The initial applications, used for measuring the average speed

in single vessels, were determined through the estimation of the frequency shift of the light backscattered by the red blood cells in the flowing stream (Tanaka & Benedek, 1974). Their development and commercialization started with the prototype designed by Stern *et al.* to monitor skin blood flow rate (Stern et al., 1977) and with the study regarding the application of LDV in microvascular tissue by Bonner & Nossal (Bonner & Nossal, 1981). The light penetrating the tissue is backscattered by red blood cells moving in different directions and with various velocities. Therefore, the backscattered light shows a frequency shift, measurements are based on the changes of the power spectrum of the backscattered light. In the years during and following the above reported two researches, LDV has been used for several medical applications in the following briefly described.

The *in vivo* monitoring of blood flow in the optical nerve head, the sub-foveal choroid, and the iris is performed with the following aims: scientific (research about the vascularization of the optical nerve), clinical (allowing to evaluate alterations in blood flow), and to quantify the effect of medical therapies in pathologic conditions (Riva et al., 2010). Riva *et al.* introduced this technique to measure blood flow in the optical nerve (Riva et al., 1982). An important innovation that allows to simplify the alignment between the measurement systems and the patient's eye was introduced by Geiser *et al.* (Geiser et al., 1999).

This technique was introduced by Shepherd and Riedel in the measurement of intestinal mucosal blood flow (Shepherd & Riedel, 1982). The measurement system consisted on a probe in contact with the tissue placed at the distal extremity of two optical fibers. The former conveyed the light, emitted by a helium-neon laser, investing a small area of intestinal tissue, the second carried the backscattered light from the tissue to a photodetector. The backscattered light produces a spectrum of frequencies (from 0 Hz to 20 kHz) analyzed in real time that provides the output of the system. Further *in vivo* trials were realized by Kiel *et al.* with valuable results (Kiel et al., 1985).

LDV was also applied to monitor blood flow in some other anatomical sites such as cerebral blood flow (Skapherdinsson et al., 1988), hepatic blood flow (Arvidsson et al., 1988), renal blood flow, gingival blood flow, and bone blood flow.

5. Conclusion

In this chapter we wanted to give an idea of the potentialities of FOSs in medical applications without pretending to be exhaustive. Intentionally we avoided to mention FOSs dedicated to monitor physiological parameters such as blood or gastric pH, blood and respiratory oxygen and carbon dioxide, bilirubin concentration and other chemical variables. Although, also in these fields, the diffusion of FOSs is far to be negligible.

The design of new fiber-based sensors is a rather active area of research with a number of possibilities to be discovered in the near future.

As professionals working in the biomedical engineering field we would emphasize that medical practitioners do not have the experience, neither the time, to carefully handle an optical-fibre sensor, above all in emergency situations. One of the greatest challenge for the optical-fibre-sensor industry is therefore to offer 'plug and play' devices that are easy to use and tolerant to rough handling. Moreover, also the cost of the necessary instrumentation should be strongly reduced.

Application-oriented customizations, reduced costs and robust designs are important for the commercial success of such sensing technology, especially for the medical market.

6. Acknowledgment

This work has been carried out under the financial support of Regione Lazio in the framework of the ITINERIS2 project (CUP code F87G10000120009).
Authors gratefully acknowledge ITAL GM s.r.l. for the precious support provided.
Authors would like to thank Ms. Sonia Rubegni for her precious collaboration in the realization of figures.

7. References

Al-Tamimi, Y. Z.; Helmy, A.; Bavetta, S. & Price, S. J. (2009). Assessment of zero drift in the Codman intracranial pressure monitor: a study from 2 neurointensive care units. *Neurosurgery*, Vol. 64, No. 1, pp. 94-98

Arvidsson, D.; Svensson, H. & Haglund U. (1988). Laser-Doppler flowmetry for estimating liver blood flow, *American Journal of Physiology, Gastrointestinal and Liver Physiology*, Vol. 254, No. 4, pp. G471-G476.

Babchenko, A.; Khanokh, B.; Shomer Y. & Nitzan N. (1999). Fiber optic sensor for the measurement of respiratory chest circumference changes. *Journal of Biomedical Optics*, Vol. 4, No. 2, pp. 224-229.

Beckwith, T. G.; Marangoni, R. D. & Lienhard, J. H. (1995). *Mechanical Measurements* (Fifth Edition), Addison-Wesley publishing Company, Inc., ISBN: 0-201-56947-7, United States of America.

Bonner, R. & Nossal, R. (1981). Model for laser Doppler measurements of blood flow in tissue, Applied Optics, Vol. 20, no. 12, pp. 2097-2107.

Bratton, S. L. et al. (2007). Intracranial pressure monitoring technology. *Journal of Neurotrauma*, Vol. 24, No. 1, pp. S45- S54.

Ceyssens, F.; Driesen, M.; Wouters, K.; Puers, R. & Leuven, K. U. (2008). A low-cost and highly integrated fiber optical pressure sensor system. *Sensors Actuators A: Physical*, Vol. 145-146, pp. 81-86.

Chavko, M.; Koller, W. A.; Prusaczyk, W. K. & McCarron, R. M. (2007). Measurement of blast wave by a miniature fiber optic pressure transducer in the rat brain. *Journal of Neuroscience Methods*, Vol. 159, No. 2, pp. 277-281.

Crutchfield, J. S.; Narayan, R. K; Robertson, C. S. & Michael, L. H. (1990). Evaluation of fiber optic intracranial pressure monitoring. *Journal of Neurosurgery*, Vol. 72, No. 3, pp. 482-487.

Davis, C.; Carome, E. F.; Weik, M. H.; Rzekiel, S. & Einfig, R. E. (1982). *Fiberoptic sensor technology handbook*, Optical Technologies Inc., Herndon.

Dehdia, J. D.; Chakravarthy K. R. N. & Ahmed A. A. (2008). Intra aortic Balloon Pumping (IABP): past, present and future. *Indian Journal of Anaesthesia*, Vol. 52, No. 4, pp. 387-391.

Ding, Y; Chen, N.; Chen, Z.; Pang, F.; Zeng, X. & Wang, T. (2010). Dynamic temperature monitoring and control with fully distributed fiber Bragg grating sensor, *Proceedings of SPIE*, *Optics in Health Care and Biomedical Optics IV,* Vol. 7845, Beijing, China.

Fabry, C. & Perot. A. Measure de petites epaisseurs en valeur absolue. *Academie des sciences*, Paris, Comptes Rendus, 1898.

Geiser, M. H.; Dierman, U. & Riva, C. E. (1999). Compact laser Doppler choroidal flowmeter, *Journal of Biomedical Optics*, Vol. 4, No. 4.

Grattan, K. T. V. & Sun, T. (2000). Fiber optic sensor technology: an overview. *Sensors and Actuators A: Physical*, Vol. 82, No 1-3, pp. 40-61.

Gurkan, D., Starodubov, D. & Yuan, X. (2005). Monitoring of the heartbeat sounds using an optical fiber bragg grating sensor, *Proceedings of 4th IEEE Conference Sensors*, Irvine, Ca.

Guttmann, J.; Kessler, V.; Mols, J.; Hentschel, R.; Hoberthur, C. & Geiger, K. (2000). Continuous calculation of intratracheal pressure in the presence of pediatric endotracheal tubes. *Critical Care Medicine*, Vol. 28, No. 4, pp. 1018-1026.

Haines, D.E. (1991). Determinants of lesion size during radiofrequency catheter ablation: the role of electrode-tissue contact pressure and duration of energy delivery. *Journal of Cardiovascular Electrophysiology*, Vol. 2, No. 6, pp. 509-515.

Hamel, C. & Pinet, E. (2006). Temperature and pressure fiber-optic sensors applied to minimally invasive diagnostics and therapies. *Progress in Biomedical Optics and Imaging*, Vol. 7, No. 6, ISSN: 1605-7422.

Hansen, T. E. (1983). A fiber optic micro-tip pressure transducer for medical applications. *Sensors and Actuators*, Vol. 4, pp. 545-554.

Hill, K. O.; Fujii, Y.; Johnson, D.C. & Kawasaki, B. S. (1978). Photosensitivity in optical fiber waveguides: application to reflection filter fabrication, *Applied Physics Letters*, Vol. 32, No. 10, pp. 647–649, 0003-6951.

Iordachita, I.; Sun, Z.; Balicki, M.; Kang, J.U.; Phee, S.J.; Handa, J.; Gehlbach, P. & Taylor R. (2009). A sub-millimetric, 0.25 mN resolution fully integrated fiber-optic force-sensing tool for retinal microsurgery. *International Journal of Computer Assisted Radiology and Surgery*, Vol. 4, No. 4, pp. 383-390.

Kiel, G. W.; Riedel, G. L.; Di Resta, G. R. & Shepherd, A. P. (1985). Gastric mucosal blood flow measured by laser-Doppler velocimetry, *American Journal of Physiology, Gastrointestinal and Liver Physiology*, Vol. 249, No. 4, pp. G539-G545.

Lee, B. (2003). Review of the present status of the optical fiber sensors. *Optical Fiber Technology*, Vol. 9, No. 2, pp. 57-79.

Lekholm, A. & Lindstrom, L. (1969). Optoelectronic transducer for intravascular measurements of pressure variations. *Medical & Biological Engineering*, Vol. 7, No. 3, pp. 333-335.

Li, C.; Chen, N.; Chen, Z. & Wang, T. (2009). Fully distributed chirped FBG sensor and application in laser-induced interstitial thermotherapy, *Proceedings of SPIE, Communications and Photonics Conference and Exhibition*, Vol. 7634, ISBN: 978-1-55752-877-3, Shanghai, China.

Meltz, G.; Morey, W. W. & Glenn, W. H. (1989). Formation of Bragg gratings in optical fibre by a transverse holographic method, *Optics Letters*, Vol. 14, No. 15, pp. 823–825.

Mignani, A. G. & Baldini, F. (1995). In-vivo biomedical monitoring by fiber-optic systems. *Journal of Lightwave Technology*, Vol. 13, No. 7, pp. 1396-1406.

Mishra, V.; Singh, N.; Tiwari, U. & Kapur, P. (2011). Fiber grating sensors in medicine: current and emerging applications. *Sensors and Actuators A: Physical*, Vol. 167, No. 2, pp. 279-290.

Mitchell, G. L. A review of Fabry-Perot interferometric sensors. Optical Fiber Sensors. *Proceedings of the 6th International Conference*, Paris, 1989.

Ostrup, R. C.; Luerssen, T. G.; Marshall, L. F. & Zornow, M. H. (1987). Continuous monitoring of intracranial pressure with miniaturized fiber optic device. *Journal of Neurosurgery*, Vol. 67, No. 2, pp. 206-209.

Peatross, J. & Ware, M. (2008). Multiple parallel interfaces, In: *Physics of Light and Optics*, pp. 141-155, http://optics.byu.edu/BYUOpticsBook_Fall2008.pdf

Petkus, V.; Ragauskas, A. & Jurkonis, R. (2002). Investigation of intracranial media ultrasonic monitoring model. *Ultrasonics*, Vol. 40, No. 1-8, pp. 829-833.

Pinet, E. Medical applications: saving lives. (2008). *Nature Photonics*, Vol. 2, pp. 150-152.

Pinet, E.; Pham, A. & Rioux, S. (2005). Miniature fiber optic pressure sensor for medical application: an opportunity for intra-aortic balloon pumping (IABP) therapy. *Proceedings of SPIE*, 17th International Conference on optical Sensors , Vol. 5855, pp. 234-237.

Puangmali, P.; Althoefer, K. & Seneviratne L. D. (2010). Mathematical model of intensity modulated bent-tip optical fiber displacement sensors. *IEEE Transactions on Instrumentation and Measurement*, Vol. 59, No. 2, pp. 283- 291.

Rao, Y. J. (1998). Fiber Bragg grating sensors: principles and applications, In: *Grattan, K.T.V. & Meggitt, B. T. (Eds.), Optical Fiber Sensor Technology*, Vol. 2, pp. 355–380, Chapman & Hall, ISBN 0 412 78290 1, London, U.K.

Rao, Y. J.; Webb, D. J.; Jackson, D.A.; Zhang, L. & Bennion, I. (1998). Optical in-fiber bragg grating sensor systems for medical applications. *Journal of Biomedical Optics*, Vol. 3, No. 1, pp. 38-44.

Riva, E. C.; Geiser, M. & Petrig, B. L. (2010). Ocular blood flow assessment using continuous laser-Doppler flowmetry, *Acta Ophthalmologica*, Vol. 88, No. 6, pp. 622-629

Riva, E. C.; Grunwald, G. E. & Sinclair, S. H. (1982). Laser Doppler measurement of relative blood velocity in the human optic nerve head, *Investigative Ophthalmology & Visual Science*, Vol. 22, No. 2, pp. 241-248.

Rolfe, P.; Scopesi, F. & Serra, G. (2007). Advances in fiber-optic sensing in medicine and biology. *Measurement Science and Technology*, Vol. 18, No. 6, pp. 1683-1688.

Shepherd, A. P. & Riedel, G. L. (1982). Continuous measurement of intestinal mucosal blood flow by laser-Doppler velocimetry, *American Journal of Physiology, Gastrointestinal and liver Physiology*, Vol. 242, No. 6, pp. G668-G672.

Shimbles, S.; Dodd, C.; Banister, K.; Mendelow, A. D. & Chambers, I. R. (2005) Clinical comparison of tympanic membrane displacement with invasive ICP measurements. *Physiological Measurement*, Vol. 26, No. 6, pp. 197-199, 2005.

Shu, X.; Liu, Y.; Zhao, D.; Gwandu, B.; Floreani, F.; Zhang, L. & Bennion, I. (2002) Dependence of temperature and strain coefficients on fiber grating type and its application to simultaneous temperature and strain measurement. *Optics Letters*, Vol. 27, No. 9, pp. 701–703.

Skarphedinsson, J. O.; Harding, H. & Thoren, P. (1988). Repeated measurements of cerebral blood flow in rats. Comparisons between the hydrogen clearance method and laser Doppler flowmetry, *Acta Physiologica*, Vol. 134, No. 1, pp. 133-142.

Smith, M. (2008). Monitoring intracranial pressure in traumatic brain injury. *Anesthesia & Analgesia*, Vol. 106, No. 1, pp. 240-248.

Sondergaard, S.; Karason, S.; Hanson, A.; Nilsson, K.; Hojer, S.; Lundin, S. & Stenqvist, A. O. (2002). Direct measurements of intratracheal pressure in pediatric respiratory monitoring. *Pediatric Research*, Vol. 51, No. 3, pp. 339-345.

Song, H.; Kim, K.; Suh, J. & Lee. (2009). Development of optical FBG force measurement system for the medical application, *Proceedings of SPIE*, Vol. 7522, Singapore, November, 2009.

Steiner, L. A. & Andrews, P. J. D. (2006). Monitoring the injured brain: ICP and CBF. *British Journal of Anaesthesia*, Vol. 97, No. 1, pp. 26-38.

Stern, M. D. et al. (1977). Continuous measurement of tissue blood flow by laser-Doppler spectroscopy, *American Journal of Physiology, Heart and Circulatory Physiology*, Vol. 232, No. 4, pp. H441-448.

Tanaka, T. & Benedek, G. (1974). Measurement of velocity of blood flow (in vivo) using a fiber optic catheter and optical mixing spectroscopy, *Applied Optics*, Vol. 14, No. 1, pp. 186-196.

Totsu, K.; Haga, Y. & Esashi M. (2005). Ultra-miniature fiber-optic pressure sensor using white light interferometry. *Journal of Micromechanics and Microengineering*, Vol. 15, No. 1.

Trost, G. C. & Hillis, L. D. (2006). Intra-aortic balloon counterpulsation. *The American Journal of Cardiology*, Vol. 97, No. 9, pp. 1391-1398.

Udd, E. (2006). *Fiber optic sensors*, John Wiley & Sons, Inc., ISBN-13 978-0-470-06810-6, Hoboken, New Jersey.

Wald, A.; Post, K.; Ransohoff, J., Hass, W. & Epstein, F. (1977). A new technique for monitoring epidural intracranial pressure. *Medical Instrumentation*, Vol. 11, No. 6, pp. 352-354.

Webb, D. J.; Hathaway, M. W. & Jackson, D. A. (2000). First in-vivo trials of a fiber Bragg grating based temperature profiling system. *Journal of Biomedical Optics*, Vol. 5, No. 1, pp. 45-50.

Wolthuis, R. A.; Mitchell, G. L.; Saaski, E.; Hartl, J. C. & Afromowitz, M. A. (1991). Development of medical pressure and temperature sensors employing optical spectrum modulation. *IEEE Transactions on Biomedical Engineering*, Vol. 38, No. 10, pp. 974-981, ISSN: 0018-9294.

Wolthuis, R. A.; Mitchell, G. L.; Hartl, J. C. & Saaski, E. (1993). Development of a dual function sensor system for measuring pressure and temperature at the tip of a single optical fiber. *IEEE Transactions on Biomedical Engineering*, Vol. 40, No. 3, pp. 298-302, ISSN: 0018-9294.

Wroblewski, D. J. & Skuratovsky, E. (1985). Vortex shedding flowmeter with fiber optic sensor. In: *31st International Instrumentation Symposium*, San Diego, CA, pp. 653-656.

Xu, M. G.; Archambault, J. L.; Reekie, L. & Dakin, J. P. (1994). Thermally-compensated bending gauge using surface mounted fiber gratings. *International Journal of Optoelectronics*, Vol. 9, pp. 281–283.

Yokoyama, K.; Nakagawa, H.; Shah, D. C.; Lambert, H.; Leo, G.; Aeby, N.; Ikeda, A.; Pitha, J. V.; Sharma, T.; Lazzara, R. & Jackman, W.M. (2008). Novel contact force sensor incorporated in irrigated radiofrequency ablation catheter predicts lesion size and incidence of steam pop and thrombus. *Circulation: Arrhythmia and Electrophysiology*, Vol. 1, pp. 354-362.

Yoshino, T.; Kurosawa, K.; Itoh, K. & Ose, T. (1982a). Fiber- optic Fabry-Perot interferometer and its sensor applications. *IEEE Journal of Quantum Electronics*, Vol. 18, No. 10, pp. 1624- 1633, 0018-9480.

Yoshino, T.; Kurosawa, K.; Itoh, K. & Ose, T. (1982b). Fiber- optic Fabry-Perot interferometer and its sensor applications. *IEEE Transactions on Microwave Theory and Techniques*, vol. 30, No. 10, pp. 1612-1621, ISSN: 0018-9480.

You, F. T. S & Yin, S. (2002). *Fiber Optic Sensors*, Marcel Dekker, Inc., ISBN: 0-8247-0732-X, New York, NY.

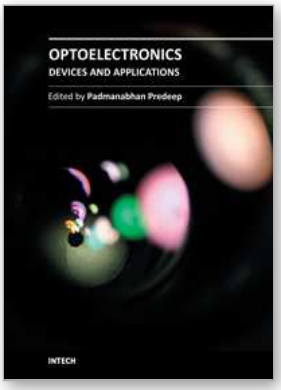

Optoelectronics - Devices and Applications

Edited by Prof. P. Predeep

ISBN 978-953-307-576-1
Hard cover, 630 pages
Publisher InTech
Published online 03, October, 2011
Published in print edition October, 2011

Optoelectronics - Devices and Applications is the second part of an edited anthology on the multifaced areas of optoelectronics by a selected group of authors including promising novices to experts in the field. Photonics and optoelectronics are making an impact multiple times as the semiconductor revolution made on the quality of our life. In telecommunication, entertainment devices, computational techniques, clean energy harvesting, medical instrumentation, materials and device characterization and scores of other areas of R&D the science of optics and electronics get coupled by fine technology advances to make incredibly large strides. The technology of light has advanced to a stage where disciplines sans boundaries are finding it indispensable. New design concepts are fast emerging and being tested and applications developed in an unimaginable pace and speed. The wide spectrum of topics related to optoelectronics and photonics presented here is sure to make this collection of essays extremely useful to students and other stake holders in the field such as researchers and device designers.

How to reference

In order to correctly reference this scholarly work, feel free to copy and paste the following:

Sergio Silvestri and Emiliano Schena (2011). Optical-Fiber Measurement Systems for Medical Applications, Optoelectronics - Devices and Applications, Prof. P. Predeep (Ed.), ISBN: 978-953-307-576-1, InTech, Available from: http://www.intechopen.com/books/optoelectronics-devices-and-applications/optical-fiber-measurement-systems-for-medical-applications

INTECH
open science | open minds

InTech Europe
University Campus STeP Ri
Slavka Krautzeka 83/A
51000 Rijeka, Croatia
Phone: +385 (51) 770 447
Fax: +385 (51) 686 166
www.intechopen.com

InTech China
Unit 405, Office Block, Hotel Equatorial Shanghai
No.65, Yan An Road (West), Shanghai, 200040, China
中国上海市延安西路65号上海国际贵都大饭店办公楼405单元
Phone: +86-21-62489820
Fax: +86-21-62489821